Jurnal Tribologi 34 (2022) 12-23

MYTRIBOS Malaysian Tribology Society

Jurnal Tribologi

Website : jurnaltribologi.mytribos.org e-issn: 2289-7232

Effect of cutting speeds on wear performance of 22MnB5 boron steel when machining with Al 6061 aluminum alloy

Mohd Fairuz Mohd Rashid [1,2], Mohd Hadzley Abu Bakar [1*], Mohd Basri Ali[1], Safarudin G. Herawan [3], Zulkifli Ahmad [4]

[1] Fakulti Teknologi Kejuruteraan Mekanikal & Pembuatan, Universiti Teknikal Malaysia Melaka, Hang Tuah Jaya, 76100 Durian Tunggal, Melaka, MALAYSIA.
[2] Bahagian Keselamatan Petroleum, Jabatan Keselamatan dan Kesihatan Pekerjaan Malaysia, MALAYSIA
[3] Industrial Engineering Department, Bina Nusantara University, INDONESIA.
[4] Teras Tegap Agrotech Sdn. Bhd., No. 60, Jalan TU2, Taman Tasik Utama, 75450 Ayer Keroh, Melaka, MALAYSIA.
*Corresponding author: hadzley@utem.edu.my

KEYWORDS

22MnB5
Tool wear
Machining
Cutting tool

ABSTRACT

22MnB5 has emerged as viable steel that possesses high strength and lightweight properties. The excellent properties for high strength and hardness application presenting capability of this material to replace high speed steel in machining medium strength alloy. In this study, quenched 22MnB5 steel with a hardness of 70 Hrc was cut into the shape of RNGN 120300 and used to machine Al 6061 aluminum alloy. Tool life and wear mechanisms were assessed at 200-350 m/min cutting speeds, 0.5 mm depth of cut and 0.1 mm/rev feed rate. The results show that machining at a 200 m/min cutting speed can achieve a maximum 861 s tool life, whereas a minimum tool life of 255 s was recorded when machining with 350 m/min cutting speed. Wear at the flank region is initiated by uniform abrasive wear before yielding to the built-up layer and built-up edge formation. The presence of molten steel in the form of a protective layer was observed in the crater region, indicating that the cutting tool was deteriorated by the adhesive wear. This study allows for a better understanding of the machining characteristics that govern 22MnB5, which may lead to more efficient 22MnB5 application in the future.

Received 5 August 2021; received in revised form 30 October 2021; accepted 12 December 2021.
To cite this article: Abu Bakar et al (2022). Effect of cutting speeds on wear performance of 22MnB5 Boron Steel when machining with Al 6061 Aluminum alloy. Jurnal Tribologi 34, pp.12-23.

1.0 INTRODUCTION

Hot stamping is a method of producing metal parts by applying high pressure and forming the part into a desired shape. In hot stamping process, blank part is heated before stamped and cooled or quenched inside specially designed dies. Several machines, including a cooling system and furnace were used in the process, which was aided by robots and conveyor systems. The simultaneous quenching and forming operation enable the stamped part committed effective microstructure transformation with less spring-back effect. When compared to conventional metal stamping, hot stamping is said to be capable of increasing the strength of steel up to four folds, reducing structural weight by using thinner sheet metal, and eliminating spring back effect. The use of hot stamped components improved the structural integrity and crash-worthiness performance of the car, allowing cars to receive 5 stars in safety assessment (Abdulhay et al., 2011 and Mori et al., 2017).

In hot stamping application, Boron alloy 22MnB5 is preferable as main material. 22MnB5 have malleable quality with thinner part is typically prepared in sheet metal form to permit weight savings of 30% to 50% when compared to commonly steels that used in commercial vehicles. The default microstructure of Boron alloy 22MnB5 was appeared to be in dominant ferrite condition (Karbasian and Tekkaya, 2010). When heated to austenitic temperature, the microstructures will be transformed into austenite phase with thermal softening condition. The heated part then transferred inside the stamping dies, to commit stamping operation. Since the dies equipped with cooling channel, the part simultaneously quenched to form and solidified into required shape. The microstructure of stamped part was changed into martensite, which offers high strength and better hardness as compared to untreated steel (Mori and Okuda, 2010 and Covusoglu et al. 2020).

The dimensional accuracy and mechanical properties of hot stamped 22MnB5 were strongly dependent on the part pressing parameters and design of hot stamping dies. Significant pressing parameters such as die force is important to stroke the blank part with full energy whilst controlled design features such as sharp edge and angles affected the final shape and spring back effect of stamped part. In addition, efficient hot stamping process also affected by quenching process inside the dies. The capability of a hot stamping dies to provide effective quenching was determined by the condition of cooling channel, surface roughness and thermal conductivity of the pressing dies (Abdulhay et al., 2011 and Zhu et al., 2020).

Significant material and application research on 22MnB5 has been conducted in the past, but the focus has primarily been on vehicle fabrication and bearing parts. Lara et al., (2013) discovered that when used as a vehicle chassis, the fatigue performance of 22MnB5 was dependent on the cutting edge surface quality. The cracks caused by the cutting process by stamping dies may result in burr formation and a rollover zone, reducing the fatigue resistance of the chassis joining. Nikravesh et al., (2015) investigated the microstructure evolution of bearing 22MnB5 and discovered that plastic deformation at elevated temperatures contributed to microstructure refinement and altered mechanical properties. The hardness of the finished parts was also affected by this transformation. Yao et al., (2018) investigated the rolling processing of 22MnB5 and concluded that the initial condition is important in determining microstructure evolution. An investigation on the fracture toughness properties of 22MnB5 steel sheets was conducted by Golling et al., (2019). The authors reported that the ability to form variant microstructures with different mechanical properties has allowed 22MnB5 in versatile applications for improving crash safety and on the same time provide weight reduction of automotive structure. Recently, Yao et al., (2020) demonstrated that 22MnB5 can be effectively

used as a car structure, particularly when combined with other high strength steels. The weld joining between these steels demonstrated the significance of microstructure control in the formation of efficient welding fusion. The findings revealed that the heat treatment process played a significant role in determining the mechanical in the mixed heating and cooling regime.

According to the above-mentioned literature studies, 22MnB5 Boron Steel is applicable in the automotive industry, particularly to meet the demand for high strength and lightweight structures. The high hardness and fracture toughness of 22MnB5 allowed it to be used in aggressive operations such as hard friction, fatigue, and thermal stresses. These advantages can be exploited in other applications where the strong and hard structure of 22MnB5 can be used to shear another softer material, specifically for machining operation. The use of 22MnB5 as cutting tool would allow possible alternative to High-Speed Steel, the common cutting tool for machining operation. In this study, 22MnB5 Boron steel was innovated to be used as a cutting tool because its refractory conditions may be useful in aggressive material removal operations. 22MnB5 Boron Steel has been prepared in the form of round insert to machine Al 6061 Aluminum Alloy at variant cutting parameters. The wear area of worn cutting tools being observed for further investigation of their failure mechanisms. This study allows for a better understanding of the machining characteristics that govern 22MnB5, which may lead to more efficient 22MnB5 Boron Steel application in the future.

2.0 EXPERIMENTAL PROCEDURE

Figure 1 depicts the original state of quenched 22Mnb5 obtained through the hot stamping process. The chemical properties of 22Mnb5 are shown in Tables 1. To convert 22Mnb5 metal sheet into cutting tool, a laser cutting machine (Figure 2) was used to cut 22m\Mnb5 sheet into RNGN 120300 tool insert. CRDN252543 tool holder was used to clamp the insert for the machining trials.

(a) (b)

Figure 1: (a) Quenched 22MnB5 boron steel (b) Laser cutting machine

(a) (b)

Figure 2: (a) Illustration of laser cutting 22MnB5 into RNGN 120300 insert (b)Sample product of 22MnB5 component being cut from hot stamped part (12 mm diameter, 3 mm thickness)

Table 1: Chemical composition of 22MnB5 boron steel (wt%) (Yao et al., 2018)

C	Mn	Si	Cr	Al	Ti	P	B	S	Fe
0.22	1.25	0.28	0.23	0.03	0.02	0.01	0.003	0.005	Bal.

The 22MnB5 tool was then used to machine the Al 6061 aluminum alloy by using CNC turning machine shown in Figure 3. The tests were carried out in wet condition in the form of conventional overhead coolant. The cutting speeds were varied between 200-350 m/min with each of individual feed rate and depth of cut were kept consistent at 0.1 mm/rev and 0.5 mm, as summarized in Table 2. Tables 3 and Table 4 show the mechanical properties and chemical composition of Al 6061 aluminum alloy respectively. Tool maker microscope was employed to measure tool wear. Wear mechanism at the contacted area was observed by Scanning Electron Microscope (SEM). EDX analysis was used to examine material transfer on top of cutting tool.

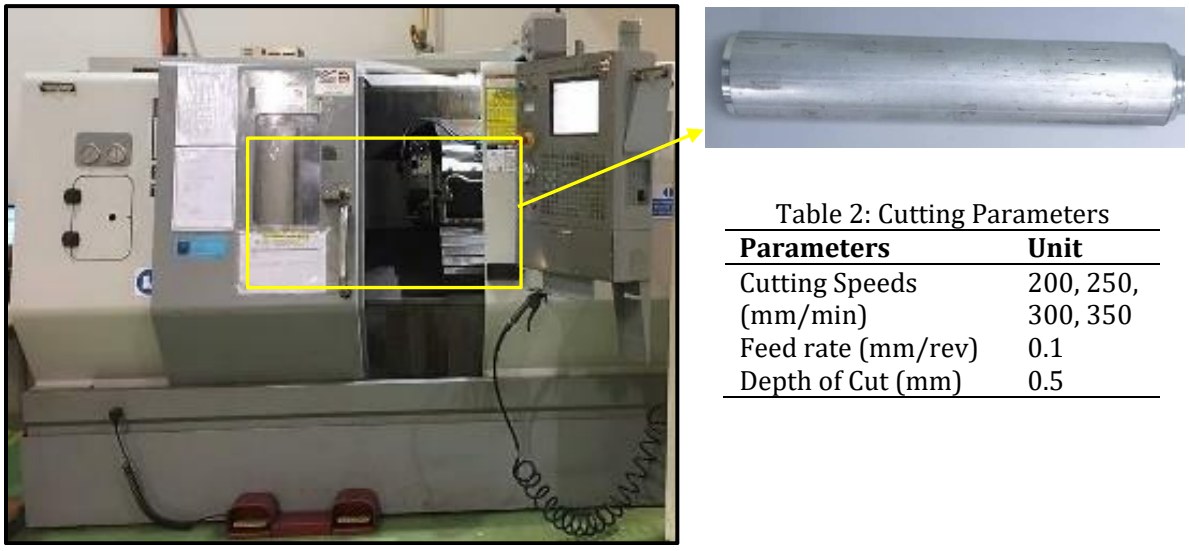

Table 2: Cutting Parameters

Parameters	Unit
Cutting Speeds (mm/min)	200, 250, 300, 350
Feed rate (mm/rev)	0.1
Depth of Cut (mm)	0.5

Figure 3: Set Up for machining tests

Table 3: Mechanical Properties Aluminium Alloy 6061 (Khan et al., 2019)

Young's Modulus	72 Gpa
Poisson's Ratio	0.3
Density (kg/m3)	27800
Yield Stress (GPa)	319 Mpa
Shear Modulus (GPa)	27
Hardness (HV)	110

Table 4: Chemical composition of Al 6061 (wt%) (Khan et al., 2019)

Cu	**Mg**	**Si**	**Fe**	**Si**	**Cr**	**Al**
0.12	1.0	0.28	0.7	0.5	0.04	Bal.

3.0 RESULTS AND DISCUSSION

Figure 4 depicts the effects of cutting speeds on flank wear for a 22MnB5 boron steel cutting tool at a feed rate of 0.10 mm/rev. Machining at a cutting speed of 200 m/min shows a linear trend in tool wear development, indicating a smooth machining process until it reached tool life at 861 s. When machining was held at 250 m/min, wear slightly increased in the early stages of machining before becoming more stable as the machining prolonged, reaching 686 s tool life. Similar to the cutting speed of 300 m/min, tool wear spiked during the initial machining and gradually stabilized to record tool life at 610 s. Machining at the highest cutting speed of 350 m/min demonstrated high tool wear within a short time of machining trials and was gradually increased to perform a short machining period of 255 s.

Figures 5(a) shows worn cutting tool images for flank wear at the lower cutting speed of 200 m/min. Uniform flank wear with grooves formation were observed. In the flank wear area, there is evidence of ridge formation along the flank surface, which reflects the formation of abrasive wear. Figure 5(b) represents abrasive wear evidenced by minor ridge formation and particle debris. Abrasion occurs when hard particles rub against the cutting tool, resulting in the formation of grooves on the contacted surfaces. Hard particles can come from two sources, which are Boron Steel detachment particles from cutting tool or chip detachment from workpiece thermal softening (Abd Maleque et al., 2017 and Liew et al., 2019). Detachment particles from Boron Steel could be obtained by gradually losing material due to tribological actions caused by two-body frictions. As the sliding continues, this particle debris may become entrapped at the tool-chip interface, resulting in severe material removal.

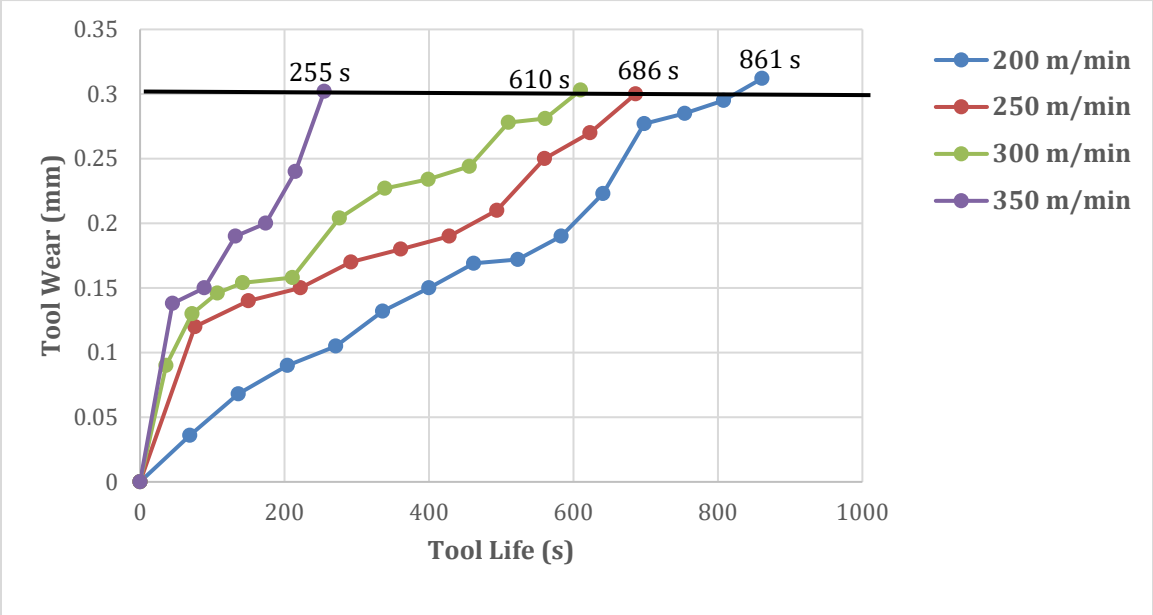

Figure 4: Effects cutting speeds on flank wear for 22MnB5 boron steel cutting tool at the 0.1 mm/rev feed rate and 0.5 mm depth of cut

In addition, abrasive wear also can be caused by compacted galling from molten Al 6061 that has attached to and accumulated on the tool surface. Detachment of Al 6061 chip could be obtained from inherent shearing of cutting tool to softened workpiece and may become trapped at the tool-chip and tool-work piece interfaces. Such detachment chip could be refractory enough to perform ploughing action on the cutting tool's surface, rubbing the surface and leaving small scars in the form of ridges (Venema et al., 2018 and Zuo et al., 2020).

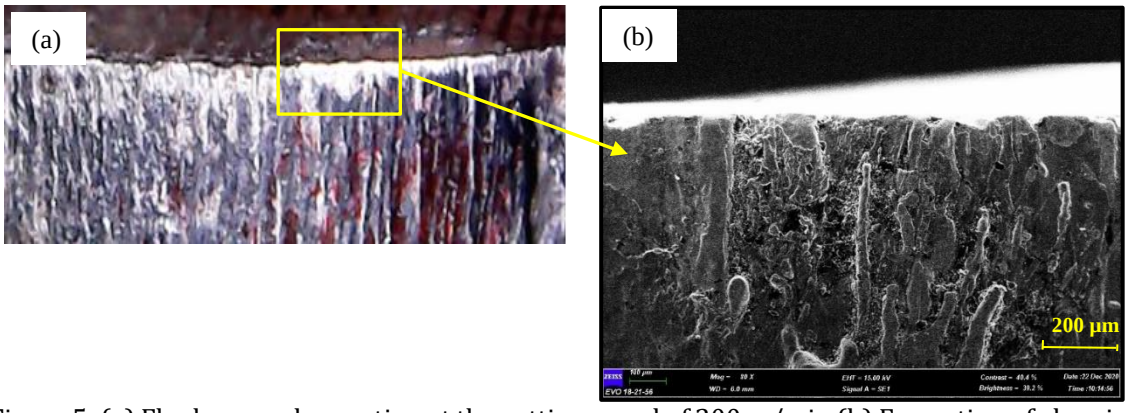

Figure 5: (a) Flank wear observation at the cutting speed of 200 m/min (b) Formation of abrasive wear which appeared in minor formation of ridges and scars

Figure 6(a) shows worn cutting tool images for flank wear at the higher cutting speed of 350 m/min. Further observation of the selected area revealed there is sign of material attachment

on the flank face that alter the edge of cutting tool as shown in Figure 6(b). Some studies in the literature have reported that this result can be attributed to the formation of chip weld that adherence on the flank surface (Sirtuli et al., 2019 and Junge et al., 2020). Chip weld is an adhered material that pours to wider areas in the form of layer on the tool's rake face. During cutting tool-workpiece material engagement, partition of AL 6061 chip may trap at the tool-chip and tool workpiece interfaces, assisted by the high pressure and pressure. Since the machining was held at higher cutting speed of 350 m/min, the trapped chip was pressurized in the form of welded layer to the tool insert, forming an attached structure at the tool nose radius's edge in the form of layer. Such a structure changed the tool nose radius, resulting in instabilities in cutting force and interfering with the contact between the cutting tool and the work piece (Wahab et al., 2015 and Parida et al., 2019). Consequently, the cutting tool is unable to effectively shear the work piece, resulting in a smeared surface and the formation of another welded layer on the machine surface.

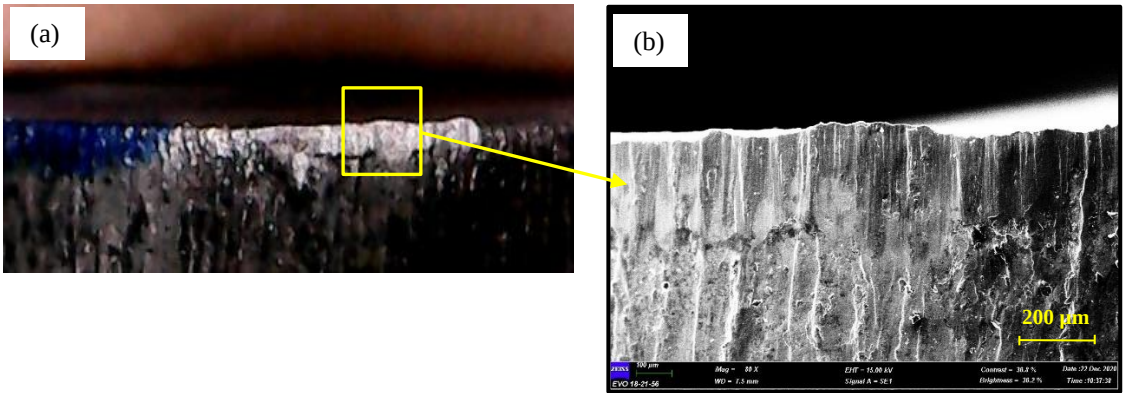

Figure 6: (a) Flank wear observation at the cutting speed of 350 m/min. (b) Indication of chip weld formations on the cutting edge of 22MnB5

Figure 7(a) and Figure 8(a) show the observation of crater area on the cutting edge of 22MnB5 when machined at 200 m/min and 350 m/min respectively. The formation of an adhesive molten aluminum layer in the form of a lamellar layer was observed in the crater area for both samples. This is true for both samples observed with EDX analysis shows that Al with 72.33 wt% (Figure 7(b)) and 43.75 wt% (Figure 8(b)) were detected on the attached layers. Large content of Al indicates that such Al elements originated from Al 6061 workpiece since the Al content in the 22MnB5 cutting tool is only 0.03 wt%. Material transfer from workpiece to tool rake face indicated that built-up edge (BUE) was formed on the crater surfaces (Ozbek et al., 2016 and Ozbek, 2020).

At a low feed rate of 0.1 mm/rev, the adherent chip is specifically covering the contact region on the crater face. Material lost within the crater wear area was contributed by layer-by-layer removal from rubbing action. At this temperature, crater formation occurred as a result of the chip alternately slipping and sticking on the rake face. Furthermore, the combination of localized temperature and dynamic friction accelerated material loss at the sliding region. Once a crater is formed, the high localized compressive stress combined with the faster traverse movement of the cutting tool plays an important role in bending the continuous chip, resulting in the formation of a discontinuous chip (Jianxin, et al., 2011 and Sarjana et al., 2020). Such molten metal existence also may result within the most noticeable sign of adhesive wear.

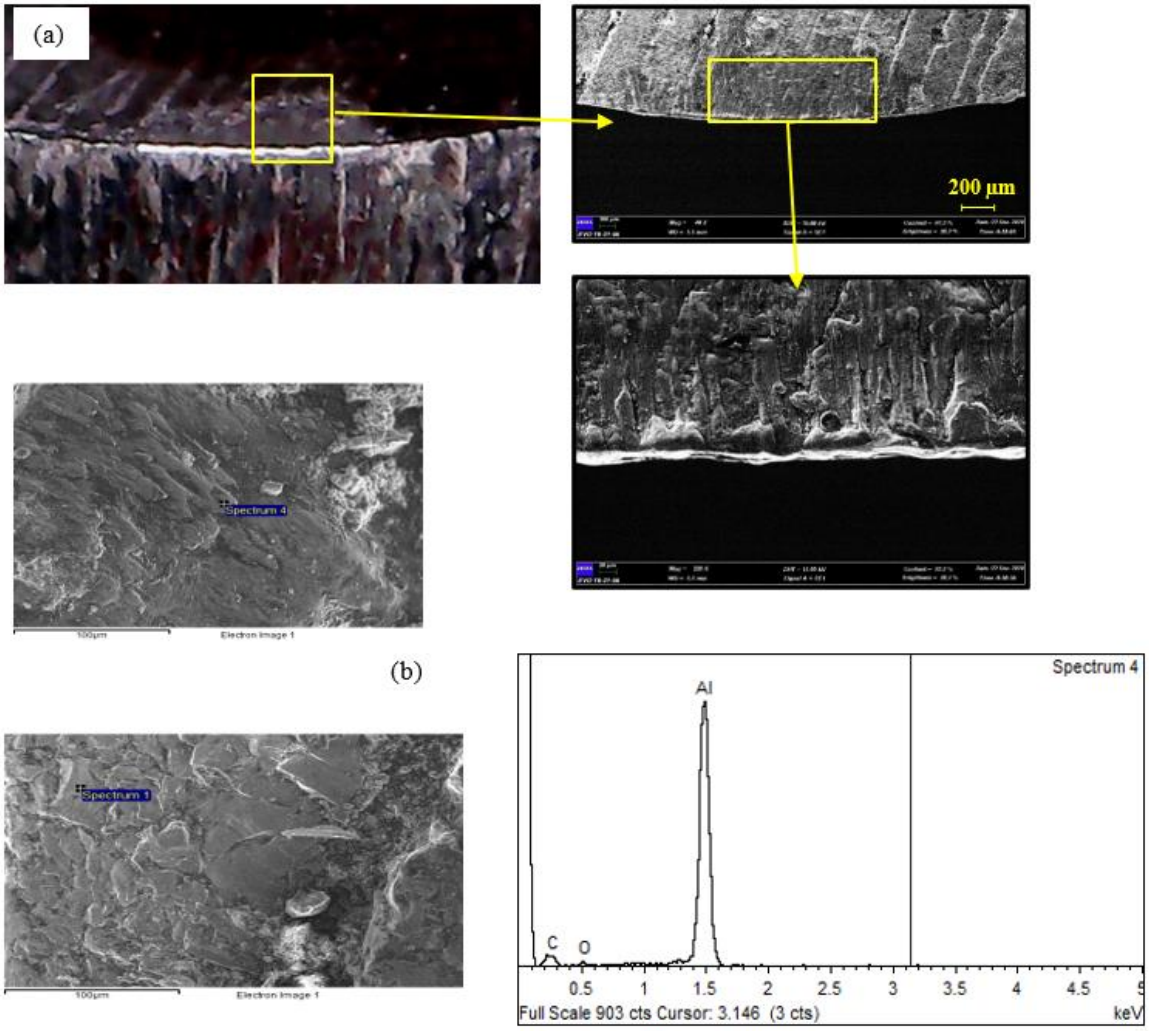

Figure 7: (a) Crater wear observation at the cutting speed of 200 m/min. (b) EDX analysis on the selected area of deposited layer

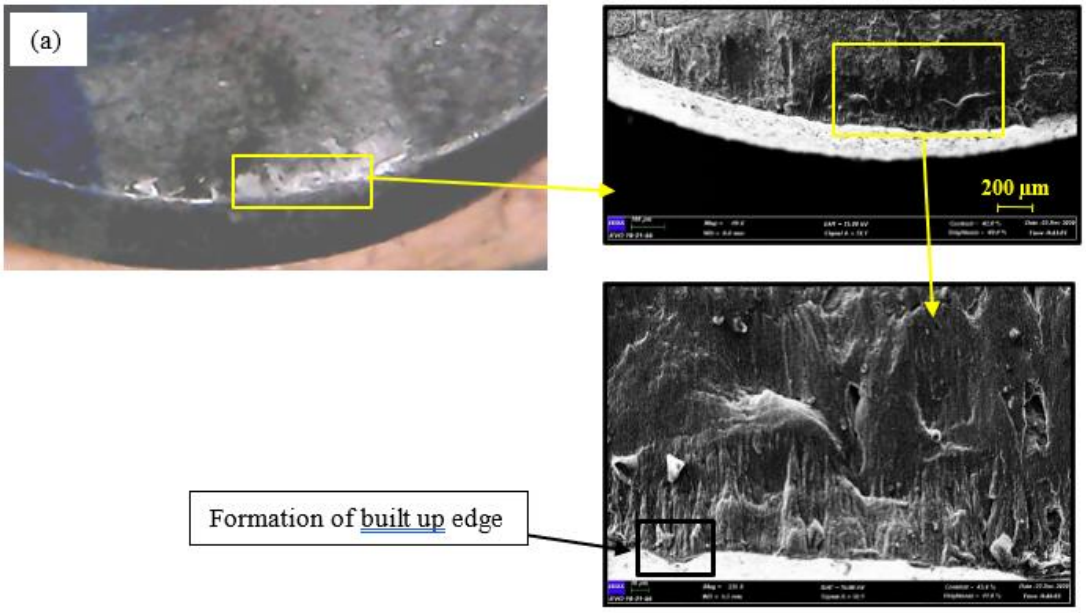

(b)

Element	Weight%
B K	0.00
C K	0.00
Al K	43.75
Si K	2.44
Fe L	53.81
Totals	100.00

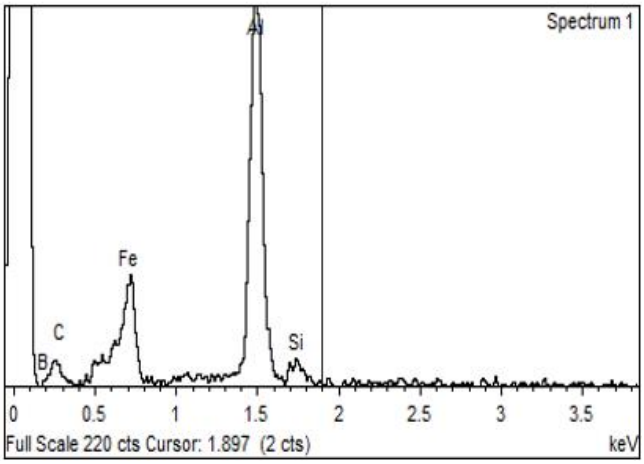

Figure 8: (a) Crater wear observation at the cutting speed of 350 m/min. (b) EDX analysis on the selected area of deposited layer

Adhesive wear could be caused by a variety of mechanisms, including smearing of adhered material, scratching, and subsequent ploughing caused by embedded Al 6061 inside the 22MnB5 microstructure. During machining, the continuous engagement and friction at the contact interfaces generated excessive heat, dissolving partial of Al 6061 underneath chips to attach on the crater face of cutting tool. At higher pressures, such attached molten chips can diffuse and dissolve through interstitial of 22MnB5 surfaces, which affected its structural integrity. As the machining chip slides on the crater face, areas on the cutting tool that affected with diffused chip started to be ploughed away, resulting in significant aggregated material loss. Accumulation of

material loss leads to critical wear at the contact zone, which accelerating tool failure throughout machining period (Ahmed et al., 2019 and Liu et al., 2020).

CONCLUSIONS

In this study, 22MnB5 Boron Steel was innovated into the application of cutting tool. Machining trials were held with Al6061 Aluminum alloy at variant cutting speeds and constant individual 0.5 mm depth of cut and 0.1 mm/rev feed rate. Wear mechanisms at various cutting parameters were examined microscopically in order to deduce the mode of tool failure. Based on the experimental results, the following conclusions can be drawn:

(a) Tool wear increased as cutting speed increased. Machining of 22MnB5 cutting tool at a lower cutting speed of 200 m/min produced the maximum tool life of 861 s. The minimum tool life of 255 s was recorded at a cutting speed of 350 m/min.
(b) The flank and crater wear dominate the failure mode of a 22MnB5 cutting tool. Rubbing action caused flank wear from the cutting edge to the flank region. Because of compressive stress and sliding chips, built-up layer and chip weld developed at the worn surfaces.
(c) An observation inside the flank area revealed that abrasive wear dominates the wear mechanism. At the rubbing interface, there was evidence of parallel lamellar ridge formation with grove formation.
(d) Adhesive wear was the dominant in the crater region. The parallel flow of molten Al 6061 can clearly be seen, which resulted from chip sliding and sticking during machining.

ACKNOWLEDGEMENT

This paper was presented at MITC202One. The authors would like to acknowledge Universiti Teknikal Malaysia Melaka (UTeM) for contribution to this project from the grant of FRGS/1/2020/FTKMP-CARE/F00438.

REFERENCES

Abd Maleque, M., Harina, L., Bello, K., Azwan, M., & Rahman M.M. (2017). Tribological properties of surface modified Ti-6Al-4V alloy under lubricated condition using Taguchi approach. Jurnal Tribologi, 17, 15-28.

Abdulhay, B., Bourouga, B., & Dessain, C. (2011). Experimental and theoretical study of thermal aspects of the hot stamping process. Applied Thermal Engineering, 31(5), 674–685.

Ahmed, Y. S., Paiva, J. M., Bose, B., & Veldhuis, S. C. (2019). New observations on built-up edge structures for improving machining performance during the cutting of superduplex stainless steel. Tribology International, 137, 212–227.

Cavusoglu, O., Cavusoglu, O., Yilmazoglu, A. G., Uzel, U., Aydin, H., & Güral, A. (2020). Microstructural features and mechanical properties of 22MnB5 hot stamping steel in different heat treatment conditions. Journal of Materials Research and Technology, 9(5), 10901–10908.

Golling, S., Frómeta, D., Casellasb, D., & Jonsén, P. (2019). Influence of microstructure on the fracture toughness of hot stamped boron steel. Materials Science and Engineering: A, 743, 529-539.

Jianxin, D., Jiantou, Z., Hui, Z., & Pei, Y. (2011). Wear mechanisms of cemented carbide tools in dry cutting of precipitation hardening semi-austenitic stainless steels. Wear, 270(7–8), 520–527.

Junge T, Liborius H, Mehner T, Nestler A, Schubert A and Lampke T (2020). Method for process monitoring of surface layer changes in turning of aluminium alloys using tools with a flank face chamfer. Procedia CIRP, 87, 432-437

Karbasian, H., & Tekkaya, A.E. (2010). A review on hot stamping, Journal of Materials Processing Technology, 210(15), 2103-2118.

Khan, M. A., Wanga, Y., Malik, A., Nazeer, F., Yasin, G., Khan, W. Q., Ahmad, T., & Zhang, H. (2019). Microstructure characterization of 7055-T6, 6061-T6511 and 7A52-T6 Al alloys subjected to ballistic impact against heavy tungsten alloy projectile. Archives of Civil and Mechanical Engineering, 19(4), 1484-1496.

Lara, A., Picas, I., & Casellas, D. (2013). Effect of the cutting process on the fatigue behaviour of press hardened and high strength dual phase steels. Journal of Materials Processing Technology, 213(11), 1908–1919.

Liew, P.J., Maisarah, K.O., Juoi, J.M., & Wang, J. (2019). Milling of Titanium Alloy using Hexagonal Boron Nitride (hBN) Nanofluid as a coolant, Journal of Advanced Manufacturing Technology, 13(3), 61-71.

Liu, E., An, W., Xu, Z., & Zhang, H. (2020). Experimental study of cutting-parameter and tool life reliability optimization in Inconel 625 machining based on wear map approach. Journal of Manufacturing Processes, 53, 34–42.

Mori, K., & Okuda, Y. (2010). Tailor die quenching in hot stamping for producing ultra-high strength steel formed parts having strength distribution. CIRP Annals - Manufacturing Technology, 59(1), 291–294.

Mori, K., Bariani, P. F., Behrens, B. A., Brosius, A., Bruschi, S., Maeno, T., Merklein, M., & Yanagimoto, J. (2017). Hot stamping of ultra-high strength steel parts. CIRP Annals - Manufacturing Technology, 66(2), 755–777.

Nikravesh, M., Naderi, M., Akbari, G. H., & Bleck, W. (2015). Phase transformations in a simulated hot stamping process of the boron bearing steel. Materials and Design, 84, 18–24.

Özbek, N. A. (2020). Effects of cryogenic treatment types on the performance of coated tungsten tools in the turning of AISI H11 steel. Journal of Materials Research and Technology, 9(4), 9442-9456.

Özbek, N. A., Cicek, A., GülesİN, M., & Özbek, O. (2016). Application of deep cryogenic treatment to uncoated tungsten carbide inserts in the turning of AISI 304 stainless steel. Metallurgical and Materials Transactions A, 47(12), 6270-6280.

Parida, A. K., Rao, P. V., & Ghosh, S. (2019). Influence of cutting speed and nose radius in the machining of Al-6061: FEM and experimental validation. Materials Today: Proceedings, 27(3), 2569–2573.

Sarjana, S. S., Bencheikh, I., Nouari, M., & Ginting, A. (2020). Study on cutting performance of cermet tool in turning of hardened alloy steel. International Journal of Refractory Metals and Hard Materials, 91, 105255.

Sirtuli L. J., Boing D. & Schroeter R. B. (2019). Evaluation of layer adhered on PCBN tools during turning of AISI D2 steel International Journal of Refractory Metals and Hard Materials, 84, 104977.

Venema, J., Hazrati, J., Matthews, D. T. A., Stegeman, R. A., & Van den Boogaard, A. H. (2018). The effects of temperature on friction and wear mechanisms during direct press hardening of Al-Si coated ultra-high strength steel. Wear, 406–407, 149–155.

Wahab, N., Inatsugu, Y., Kubota, S., Kim, S., & Sasahara, H. (2015). An Integral Method to Determine Workpiece Flow Stress and Friction Characteristics in Metal Cutting. Internationa Journal of Automation Technology, 9(6), 775-781.

Yao, S. J., Feng, L., Yang, D. L., Han, D. X., Liu, Y., Li, Q. Q., Guo, J. H., & Chao, B. J. (2018). A potential hot stamping process for microstructure optimization of 22MnB5 steels characterized by asymmetric pre-rolling and one- or two-step pre-heating. Journal of Materials Processing Technology, 254, 100–107.

Yao, S., Chen, L., Chu, G., Zhao, H., Feng, L., & Wang, G. (2020). Microstructure characterization of reversed transformation in cryogenically rolled 22MNB5. Materials, 13(7), 1741.

Zhu, B., Xu, Z., Wang, K., & Zhang, Y. (2020). Nondestructive evaluation of hot stamping boron steel with martensite/bainite mixed microstructures based on magnetic Barkhausen noise detection. Journal of Magnetism and Magnetic Materials, 503, 166598.

Zuo, J., Lin, Y., Zhong, P., Liu, Y. (2020). Investigation on adhesive wear process of tool coating surface under high-adhesive rate environment in cutting Beryllium-copper C17200 alloy, Materials Letters, 279, 128488.